JACC Vol. 30, No. 7
December 1997:1641–8

Postischemic Stunning Can Affect Left Ventricular Ejection Fraction and Regional Wall Motion on Post-Stress Gated Sestamibi Tomograms

LYNNE L. JOHNSON, MD, FACC, STEPHEN A. VERDESCA, MD, WADY Y. AUDE, MD, RITA C. XAVIER, RN, LORRAINE T. NOTT, CNMT, MICHAEL W. CAMPANELLA, MS, GUIDO GERMANO, PHD

Providence, Rhode Island

Objectives. **This study was designed to investigate whether left ventricular ejection fraction (LVEF) calculated from post-stress single-photon emission computed tomography (SPECT) reflects the basal value for LVEF or whether post-stress LVEF is reduced in some patients with stress-induced ischemia.**

Background. **Automated programs are now commercially available for assessing global left ventricular (LV) function from post-stress technetium-99m sestamibi gated SPECT performed >15 min after completion of exercise.**

Methods. **Eighty-one sequential patients who underwent a 2-day stress/rest sestamibi imaging protocol and showed perfusion defects on the post-stress tomogram underwent gated acquisition of the second-day rest tomogram. The post-stress and rest tomographic images were read for presence, location, severity and reversibility of defects by consensus of two to three experienced observers with the aid of circumferential count displays. Defects were scored as mild, moderate or severe and as completely or partially reversible or fixed, and a summed defect severity score was calculated. Of these 81 scans, 20 showed nonreversible perfusion defects (group 3), whereas 61 showed reversible perfusion defects. Post-stress and rest LVEF was calculated from the processed gated SPECT data. From 15 additional patients who underwent rest gated SPECT studies on separate days, serial reproducibility of LVEF values calculated from the gated SPECT data was determined to be ±5.2%. Coronary angiography was performed within 3 months of the scan without intervening events in 47 of 81 patients, including 39 of 61 with reversible perfusion defects.**

Results. **In 22 (36%) of 61 patients with reversible perfusion defects, post-stress LVEF was >5% lower than that at rest (group 2), whereas in the remaining 39 patients, post-stress LVEF was either ±5% or greater than that at rest (group 1). Segmental chordal shortening analysis performed in group 2 studies showed that differences in chordal shortening between rest and post-stress were significantly greater in the reversible perfusion defect territories than in the nonischemic perfusion defect territories ([mean ± SD] 0.14 ± 0.14 vs. 0.02 ± 0.09, respectively, $p < 0.0001$). There were no significant differences among groups for any of the following variables: age, gender, previous myocardial infarction and type of stress. Time to imaging and stress and scan variables were correlated with the change in LVEF by univariate analysis, and the two variables that correlated significantly were the summed defect reversibility score on the scan and a left anterior descending coronary artery location of the scan defect. Only summed defect reversibility score was significant on multivariate analysis.**

Conclusions. **When the only gated sestamibi scan is the post-stress scan, global and regional LV function will not represent basal LV function in all patients with stress-induced ischemia.**

(J Am Coll Cardiol 1997;30:1641–8)

©1997 by the American College of Cardiology

The high photon flux and long myocardial retention times of most technetium-based myocardial perfusion imaging agents allow for electrocardiographic (ECG) gating of tomographic acquisitions with computer-processed output that can be used to assess global and regional left ventricular (LV) function. Using either of the 1-day imaging protocols (a low dose/high dose sestamibi protocol or a dual-isotope rest/thallium stress sestamibi protocol), only the post-stress tomogram is usually gated. Myocardial uptake of perfusion tracer at the time of tomographic acquisition represents the relative myocardial perfusion pattern at the time of tracer injection, but the gated tomogram represents LV function at the time of acquisition, which can be anywhere from 15 min to 1 h after the completion of stress. Patients who develop stress-induced ischemia will have some component of ischemic LV dysfunction. The time course for the resolution of ischemic LV dysfunction in patients has been reported to range from immediate to 30 min (1–6). From experimental studies (7–10), depression of systolic

From the Rhode Island Hospital, Brown University, Providence, Rhode Island. This study was funded in part by a grant from DuPont Radiopharmaceuticals, North Billerica, Massachusetts.

Manuscript received December 6, 1996; revised manuscript received July 25, 1997, accepted September 2, 1997.

Address for correspondence: Dr. Lynne L. Johnson, Rhode Island Hospital, Main Building, Room 208, 593 Eddy Street, Providence, Rhode Island 02906. E-mail: lynne-johnson@brown.edu.

©1997 by the American College of Cardiology
Published by Elsevier Science Inc.

0735-1097/97/$17.00
PII S0735-1097(97)00388-4

Abbreviations and Acronyms

ECG = electrocardiogram, electrocardiographic
LAD = left anterior descending coronary artery
LV = left ventricular
LVEF = left ventricular ejection fraction
SPECT = single-photon emission computed tomography (tomographic)
Tc-99m = technetium-99m

function in the ischemic zone after periods of brief coronary artery occlusion has been demonstrated to persist for variable time periods lasting as long as 6 h. In patients with severe coronary artery stenoses or multivessel disease, repetitive episodes of ischemic stunning may lead to chronic depression in LV function (11–15). It is therefore possible that in some patients with stress-induced ischemia, LV regional and global function has not returned to baseline by the time of post-stress gated acquisition, and measuring post-stress LV ejection fraction (LVEF) in these patients would underestimate basal LVEF. Consequently, the present study was performed to investigate whether the post-stress LVEF, acquired >15 min after the completion of exercise, reflects the basal LVEF or whether it is reduced in some patients and, if so, what clinical, scan or angiographic variables are associated with a depression in post-stress segmental and global LV function.

Methods

Study patients. Ninety-one sequential patients scheduled for 2-day stress/rest sestamibi studies from May 1995 to December 1995 who had defects on their stress (day 1) study were scheduled to undergo gated acquisition on their rest (day 2) acquisition. Gating was successful on both studies in 81 patients and raw archived data were available for analysis. Of these 81 patients, 61 showed either complete or partial reversibility of stress perfusion defects, and 20 had fixed defects. There were 55 men and 6 women with a mean (±SD) age of 60 ± 11 years. Twenty-eight of 61 patients had a history of previous myocardial infarction. Treadmill stress was performed in 51 and pharmacologic stress with dipyridamole in 10. Coronary angiography was performed within 3 months of the stress perfusion study in 39 of 61 patients without an intervening cardiac event.

Stress perfusion imaging. Perfusion imaging studies were performed using one of the following protocols: 1) maximal treadmill exercise using the Bruce protocol (n = 51); or 2) pharmacologic stress (n = 10). Patients who underwent exercise treadmill testing received an injection of 18 to 27 mCi of technetium-99m (Tc-99m) sestamibi (depending on weight) at peak exercise and exercised at this level for an additional minute. Stress imaging was performed between 15 and 45 min after injection. Patients undergoing pharmacologic testing received an infusion of 0.56 mg/kg body weight of dipyridamole over 4 min. Three minutes after completion of the infusion, the dose of sestamibi was injected. Stress imaging was performed ~60 min after tracer injection. On the following day, all patients returned for the day 2 rest scans, at which time approximately the same dose of Tc-99m sestamibi was injected at rest, and imaging was performed ~60 min later.

Single-photon emission computed tomographic acquisition and processing. Single-photon emission computed tomographic (SPECT) images were acquired on a rotating dual detector gamma camera with the detectors mounted at right angles and fitted with high resolution collimators (VXHR, ADAC Vertex). Image acquisition variables were the following: a 140-keV photopeak with a 20% window; 64 projections at 25 s/projection over a 180° (90°/detector) elliptical orbit; a 38-cm roving detector mask; a matrix size 64 × 64 × 8. Acquisitions were gated for 8 frames/cardiac cycle, with 100% beat acceptance. The eight-interval projection data sets were prefiltered with a two-dimensional Butterworth filter (order 2.5, critical frequence 0.22 cycles/pixel, pixel size 0.64 cm) reconstructed with filtered backprojection (ramp filter) and no attenuation correction. The resulting transaxial image sets were reoriented into short-axis sets that were then processed in batch mode in a stand-alone workstation (Sun SPARC 5, 32 MB RAM) running the automatic LVEF quantification software. The projection data sets were also summed, prefiltered with a two-dimensional Butterworth filter (order 2.5, critical frequency 0.33 cycles/pixel, pixel size 0.64 cm), reconstructed and reoriented, producing high count short, vertical and horizontal long-axis images for qualitative interpretation and for polar plot and circumferential count displays.

LVEF was calculated using a completely automated algorithm, previously described and validated (16). The algorithm operates in the three-dimensional space and uses the gated short-axis image sets. It segments the left ventricle; estimates and displays the endocardial surface, the epicardial surface and the valve plane for every gating interval; calculates from them the endocardial and epicardial volumes; isolates the intervals corresponding to end-diastole and end-systole; and derives the related LVEF.

Scan interpretation. The post-stress and rest tomographic images were interpreted for presence, location, severity and reversibility of defects by consensus of two to three experienced observers (L.L.J., S.A.V.). Using an eight-segment model that divides the left ventricle into inferolateral, inferior, anteroseptal, anterior, anterolateral, anteroapical and inferoapical segments, defects were scored as follows: 1 = *mild*; 2 = *moderate*; 3 = *severe*; or 4 = *absent*; and as *completely reversible, partially reversible* or *fixed* on the basis of additional information from the normalized circumferential count profile display. A *summed stress defect severity score* was calculated as the sum of all defect severities on the stress scan, and a *summed defect reversibility score* was calculated as the sum of differences in scores between stress and rest for all reversible or partially reversible segments.

Segmental chordal shortening analysis. One midvertical long-axis slice and one mid short-axis slice at end-diastole and end-systole from both the post-stress and rest gated studies for the 22 patients in group 2 were exported to a SUN workstation.

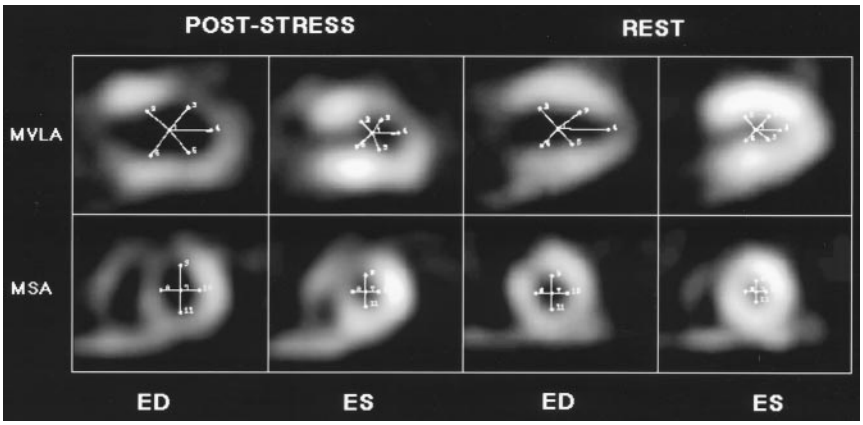

Figure 1. Example of chordal shortening method from one group 2 patient. Midvertical long-axis slices (MVLA) (**top**) and mid short-axis slices (MSA) (**bottom**) with nine segmental chords superimposed. ED = end-diastole; ES = end-systole.

Contrast was adjusted in gray scale to best identify the endocardial surface. The center of each short-axis or vertical long-axis slice was identified on the end-diastolic and end-systolic datasets, and four chords were drawn from the centroid to the endocardial surface on the short-axis (anterior, lateral, inferior and septal) and five chords from the centroid to the endocardial surface on the vertical long-axis slices (anterobasal, anteroapical, apex, inferoapical, inferobasal) (Fig. 1). Systolic shortening for all chords was calculated as end-diastolic length minus end-systolic length divided by end-diastolic length. The differences in shortening between the post-stress and the rest gated SPECT studies for all chords were calculated. The chords were assigned to either "ischemic" or "nonischemic" vascular territories on the basis of whether the perfusion images showed reversible defects corresponding in location to the respective chords. For example, the anterior and septal chords from the short-axis and the anterior and apical chords from the vertical long-axis slices were considered to be in the ischemic territory if a patient had extensive reversible anterior and anteroseptal perfusion defects (left anterior descending coronary artery [LAD] territory). Mean values for differences in chordal shortening between end-diastole and end-systole corresponding to ischemic and nonischemic regions were calculated and compared.

Serial reproducibility. Fifteen additional patients agreed to return to the laboratory for a third day as part of a study to test the serial reproducibility of LVEF calculated from the gated SPECT data. The recruitment of patients with serial reproducibility was approved by the Office of Research Administration of Rhode Island Hospital. Patients signed a written consent before their day 2 rest injection, and the rest dose was decreased to keep the total dosimetry as low as reasonably allowable. On the third day, patients returned for a second rest injection of the same dose as that received on day 2 and underwent a second rest gated SPECT acquisition. The LVEFs from the two rest gated SPECT acquisitions were calculated using the same previously described automated program. No patient in the serial reproducibility study was included in the comparison of post-stress and rest LVEFs and segmental shortening. The serial reproducibility of the gated SPECT LVEF was determined to be 5.2%, which represented ±2 SD of the mean value for the serial measurements. Ischemic patients in whom the post-stress LVEF was <5% of the rest LVEF were assigned to group 2; those with a post-stress LVEF value either within ±5% of or higher than the rest value were assigned to group 1. Patients without ischemia (fixed defects) were assigned to group 3.

Statistical analysis. Differences in demographic data among groups were tested using analysis of variance. Univariate tests were done using the Spearman rank correlation to correlate stress test, scan and coronary angiographic data with the change in LVEF for the three groups of patients. Multivariate regression analysis was performed using the variables that were significant by univariate analysis.

Results

Serial reproducibility. LVEF values for the first rest LVEF ranged from 22% to 69% and from 27% to 71% for the second rest LVEF, and when the second LVEF was plotted against the first LVEF, the regression line was not different from the line of identity (Fig. 2). The differences between the serial measurements expressed in LVEF units (not as percent of LVEF values) ranged from −3% to +5% (mean +1.0 ± 2.6%). The outside limits for serial reproducibility of the measurement were determined to be 2 SD beyond the mean value, which corresponded to a value of ±5.2%. Using the cutoff value of ±5%, 22 (36%) of 61 ischemic patients in this unselected patient cohort showed values for the post-stress LVEF calculated from the gated SPECT data <5% of the rest LVEF values (group 2). In the remaining 39 ischemic patients (group 1), the post-stress LVEF values were either within ±5% of the rest values or higher than the rest value (Fig. 3).

Clinical and test variables. The mean age was 61 ± 12 years for group 1, 60 ± 9 years for group 2 and 65 ± 11 years for group 3 (p = NS). There were 4 women and 39 men in group 1, 2 women and 22 men in group 2 and 5 women and 20 men in group 3 (p = NS). Eighteen of 39 patients in group 1, 10 of 22 in group 2 and 14 of 20 in group 3 had a history of or a previous myocardial infarction (p = NS). Stress was per-

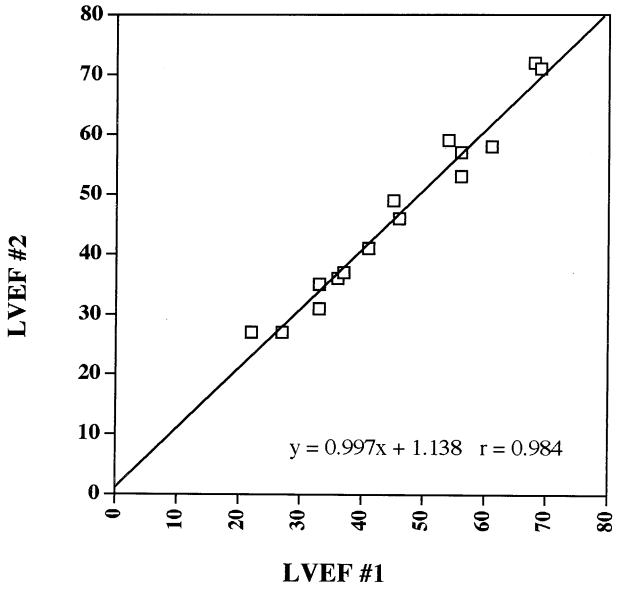

Figure 2. Serial reproducibility studies with LVEF calculated from the first gated SPECT study on the x-axis versus LVEF calculated from the second gated SPECT study on the y-axis. The regression line **(open squares)** is not significantly different from the line of identity **(solid line)**.

formed as follows: group 1 = treadmill in 35 patients, dipyridamole in 4; group 2 = treadmill in 16 patients, dipyridamole in 6; group 3 = treadmill in 16 patients, dipyridamole in 4 (p = NS). The mean time between tracer injection at peak stress and imaging was 32.5 ± 17.7 min in group 1 and 30.8 ± 21.0 min in group 2 (p = NS). For group 2 patients, the time

Figure 3. Post-stress versus rest LVEF values for groups 1 **(squares)** and 2 **(triangles)**.

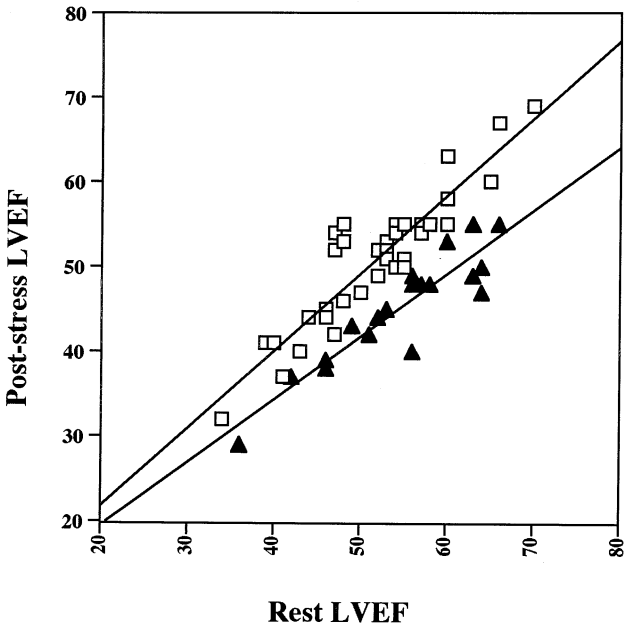

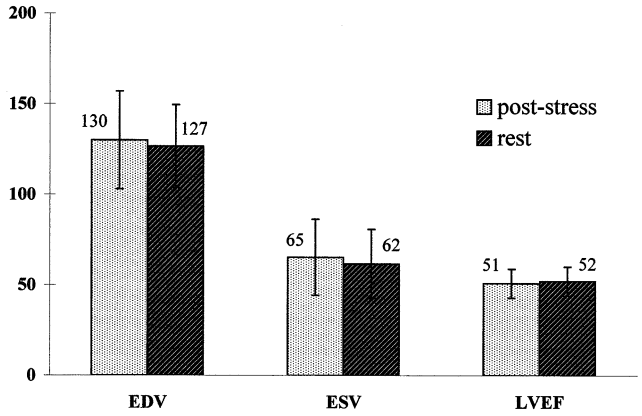

Figure 4. End-diastolic volume (EDV), end-systolic volume (ESV) and post-stress and rest LVEF for group 1 patients. **Numbers above bars** = mean value ± SD.

interval between the completion of exercise and scanning was >30 min in six patients and >60 min in three.

Group 1. Mean rest LVEF was 52 ± 8% (range 34% to 66%); mean post-stress LVEF was 51 ± 8% (range 32% to 69%). In 2 of 39 patients, the post-stress LVEF was >5% higher than the resting value (7% greater for both patients). Mean post-stress LV end-diastolic volume was 130 ± 27 ml; mean end-systolic volume was 62 ± 18 ml. Mean rest LV end-diastolic volume was 127 ± 22 ml; mean end-systolic volume was 61 ± 19 ml (Fig. 4).

Group 2. Mean rest LVEF was 56 ± 9% (range 34% to 72%); mean post-stress LVEF was 46 ± 7% (range 29% to 58%). The difference between post-stress and rest values ranged from −6% to −16%. Eight of 22 patients had a difference of ≥10% between the two studies, and 13 of 22 had a difference of ≥8% between the two studies. Mean post-stress LV end-diastolic volume was 131 ± 46 ml; mean end-systolic volume was 73 ± 36 ml. Mean rest LV end-diastolic volume was 122 ± 42 ml; mean end-systolic volume was 57 ± 33 ml (Fig. 5). An example from group 2 is shown in Fig. 6.

Figure 5. End-diastolic volume (EDV), end-systolic volume (ESV) and post-stress and rest LVEF for group 2 patients. **Numbers above bars** = mean value ± SD.

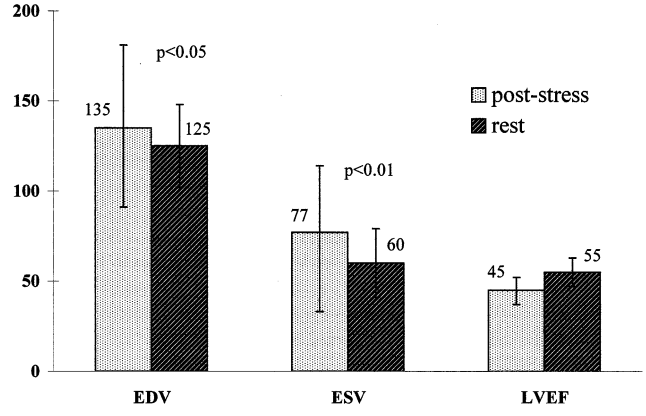

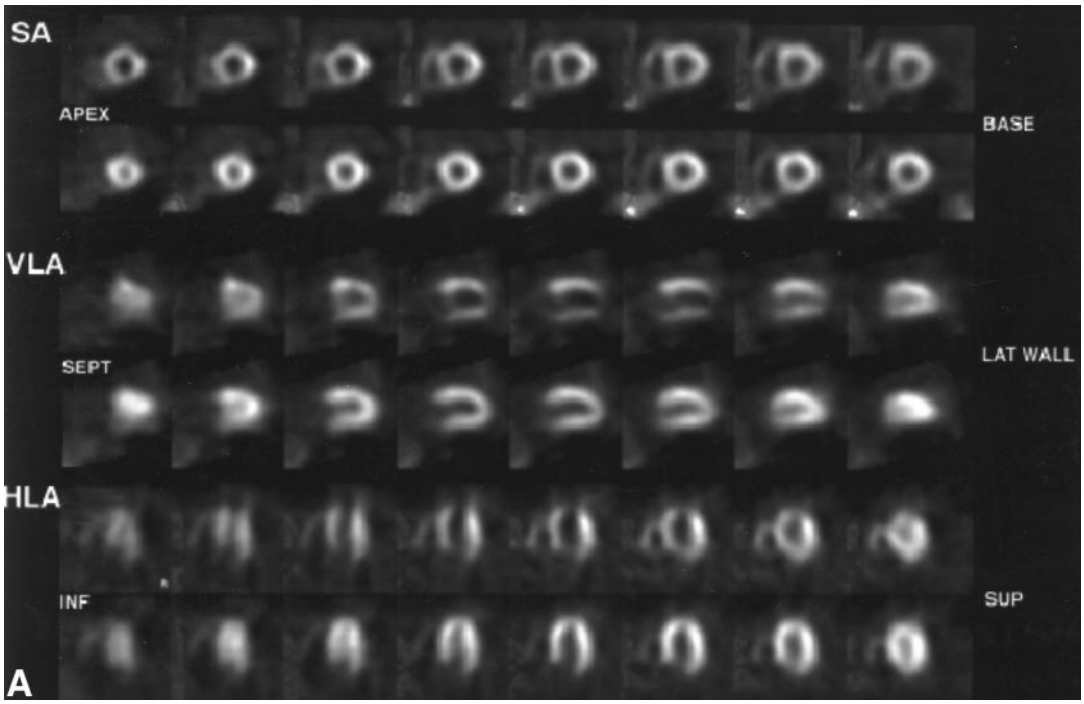

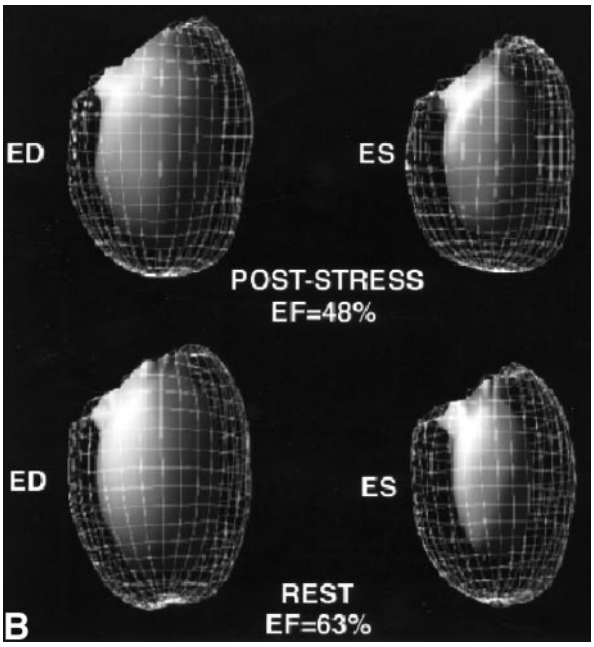

Figure 6. Panels A and **B** from a group 2 patient. **Panel A** shows the row tomographic display with the stress images displayed above the rest images for each set of slices. The short axis (SA) slices are displayed on top from apex to base (**left to right**). The vertical long-axis (VLA) slices are displayed in the middle from septum (SEPT) to lateral (LAT) wall. The horizontal long-axis (HLA) slices are displayed on the bottom from inferior (INF) to superior (SUP). The stress scans show extensive defects in two vascular territories (LAD and right coronary artery), which fill in completely on the rest scans. **Panel B** shows the three-dimensional display images from the same patient. The solid contoured image represents the LV cavity at end-diastole (ED) and end-systole (ES) and the mesh part of the image the epicardial surface. The images displayed show septum, apex and lateral walls. The end-systolic volume is noticeably larger on the post-stress study, and the LVEF of 48% is much lower than the rest value of 63%.

Fixed defects. For the 20 patients with fixed perfusion defects, mean post-stress LVEF was 42 ± 14% (range 27% to 66%), and mean rest LVEF was 41 ± 14% (range 27% to 70%). The regression line for the two sets of values was not different from the line of identity (Fig. 7). The mean difference between the two LVEF values (rest minus post-stress) was −1.1 ± 3.8% (range −10% to 4%). Two standard deviations of the mean was higher than that for the patients with serial reproducibility (7.6% vs. 5.2%). In most cases, the post-stress values were higher than the rest values. In one patient, the rest LVEF was 4% higher than the post-stress value; in the remaining patients, the difference was smaller or negative.

Chordal shortening. For group 2 patients, a total of 198 chordal segment shortenings (9/scan) were measured for both the post-stress and rest scans and were divided into those corresponding to ischemic (reversible perfusion defects) and nonischemic regions (normal regions or fixed perfusion defect territories). For the nonischemic segments, mean chordal shortening for the post-stress scan was 0.30 ± 0.12; that for the rest scan was 0.32 ± 0.13, and the difference was 0.02 ± 0.09. For the ischemic segments, the mean chordal shortening for the post-stress scan was 0.25 ± 0.14, that for the rest scan was 0.39 ± 0.14, and the difference was 0.14 ± 0.15. The difference in chordal

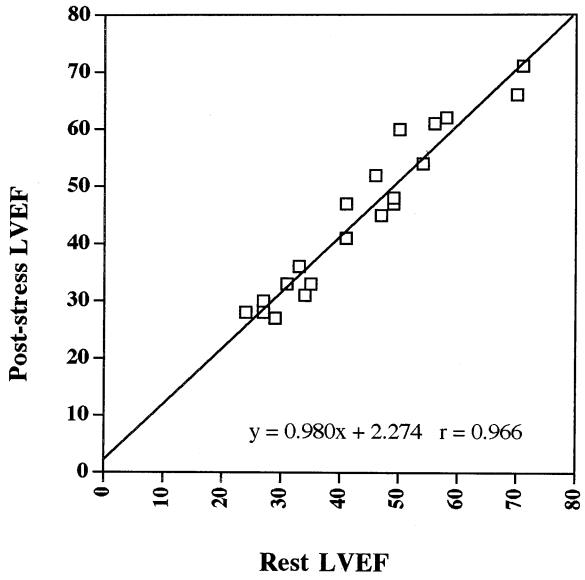

Figure 7. Post-stress versus rest LVEF values for patients with fixed perfusion defects. Symbols as in Figure 2.

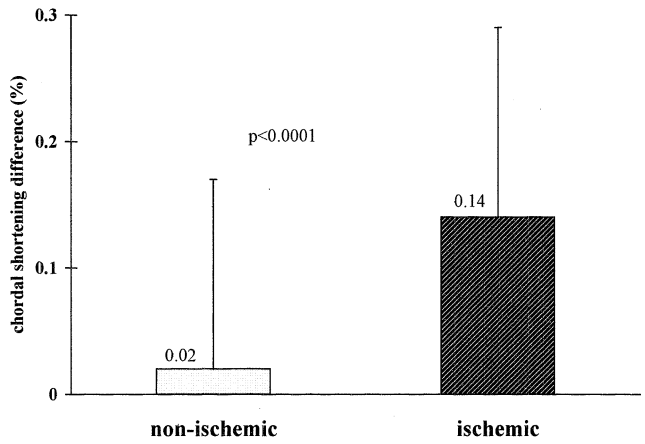

Figure 8. Differences in chordal shortening between nonischemic and ischemic segments in group 2 patients. **Numbers above bars** = mean value ± SD.

shortening was significantly greater for the ischemic than for the nonischemic segments ($p < 0.001$) (Fig. 8).

Stress and scan variables. Factors potentially affecting post-stress LVEF, including time between injection and imaging, and factors known to be associated with disease severity were examined (Table 1). Univariate analysis was performed using the change in LVEF as the independent variable, and the following dependent variables were analyzed as both continuous and dichotomous factors: time to imaging, ST segment depression, stress type, summed stress defect severity score and summed defect reversibility score, defect location, exercise time and number of diseased vessels. The two variables that correlated significantly were summed defect reversibility score ($p < 0.01$) and LAD perfusion defect location ($p < 0.01$). When multivariate regression analysis was performed, the summed defect reversibility score was significant ($p < 0.05$) but not LAD perfusion defect location.

Discussion

Information on the time course of the resolution of ischemia-induced LV dysfunction after completion of exercise in patients is limited and inconsistent. The results of some studies using imaging modalities that diagnose ischemia on the basis of transient development of regional wall motion abnormalities or fall in global LVEF suggest that ischemic LV dysfunction manifested by global depression of LV function resolves rapidly, whereas the results of other studies indicate that regional LV dysfunction may persist (1–6). Studies (1,3) using gated blood pool scanning performed during and immediately after upright or semisupine bicycle exercise in patients with coronary artery disease have found that LVEF rises during the early phases of exercise and then falls at the ischemic threshold and rises again immediately after stress. Possible factors responsible for the rise immediately after exercise include maintenance of an upright position with blood pooling in the lower extremities, leading to reduced end-diastolic volume and wall stress and positive inotropic effects of high levels of circulating catecholamines. Greater reduction in end-systolic volume found in these studies suggests that the catecholamine effect is predominant (1). However, the results of a more recent study (4) using serial gated blood pool imaging with bicycle exercise or perfusion imaging, combined with echocardiography in patients with angiographically documented coronary artery stenoses, demonstrated that in a high percentage of patients, regional dyssynergy persisted up to 2 h after completion of exercise. In addition, an echocardiographic study (5,6) was performed that showed persistence of regional wall motion abnormalities 30 min after completion of treadmill exercise in a high proportion of a small number of patients with multivessel disease.

Postischemic stunning. Postischemic stunning was first observed in animal models of occlusion and reperfusion (7,8). Either a prolonged moderately severe reduction in myocardial blood flow or repeated brief episodes of occlusion followed by reperfusion lead to periods of prolonged reduction in contraction in the risk region, in the absence of necrosis (7–10). The

Table 1. Univariate Analysis of Stress Variables

	r Coeff	p Value
Time to imaging	−0.113	0.350
Exercise time	−0.090	0.488
ST segment depression	0.212	0.101
Summed defect severity score	0.108	0.362
Summed defect reversibility score	0.300	0.009
LAD defect	0.324	0.004
RCA defect	0.146	0.210
LCx defect	0.135	0.250
No. of diseased vessels	0.550	0.680

Coeff = coefficient; LAD = left anterior descending coronary artery; LCx = left circumflex coronary artery; RCA = right coronary artery.

severity and duration of regional LV dysfunction depend on the severity of the ischemic insult as well as the metabolic condition of the myocardium before the insult (14). Both metabolic derangements as well as alterations in high energy phosphates have been demonstrated in the stunned myocardium. In reperfused dysfunctional and nonnecrotic myocardium, delayed clearance of Carbon-11 palmitic acid activity from the myocardium and increased uptake of fluorine-18 fluorodeoxyglucose have been demonstrated in an animal model using positron emission tomographic imaging (17). More directly related to the contractile mechanism, studies (18) using phosphorus magnetic resonance spectroscopy showed that the ratio of phosphocreatine to beta-adenosine triphosphate (ATP) did not return to control values with reperfusion, and a fraction of control beta-ATP levels paralleled postischemic LV dysfunction.

It has long been observed in patients with coronary artery disease that there can be a dissociation between myocardial viability (defined as the potential of the myocardium to improve function with restoration of flow with revascularization) and the extent and severity of dyssynergy (12). Mechanisms proposed for this phenomenon are either hibernation, in which LV function is downregulated to match reduced oxygen supply due to severe flow-limiting lesions, or repetitive stunning (15). The majority of patients with reversibly dysfunctional myocardium probably have repetitively stunned myocardium. A number of studies (11,13) have now demonstrated that stunning does occur in patients with coronary artery disease as a consequence of repeated episodes of either symptomatic or asymptomatic ischemia during daily life.

Present study. In the present study 22 (36%) of 61 patients with stress-induced ischemia had a post-stress LVEF, determined ~30 min after the completion of exercise, below the limits of serial reproducibility compared with the rest LVEF. Chordal shortening analysis showed that the depression in global LV function was due to depression in regional function in the territory of the reversible perfusion defect. When treadmill, angiographic and scan variables known to be associated with disease severity were correlated with presence of reduced post-stress LVEF, both the summed defect reversibility score and location of the reversible defect in the LAD territory showed a significant correlation. The failure of other stress test variables to correlate is probably due to the fact that all patients in groups 1 and 2 developed ischemia; many had abnormal results on the rest ECG; and many had a previous myocardial infarction. The failure of multivessel disease by angiography to correlate may be due to the severity of individual stenoses and to the fact that both groups had about the same proportion of patients with a previous myocardial infarction. However, these data suggest that disease severity forms the necessary condition for the occurrence of prolonged post-stress depression in LV function due to postischemic stunning.

Six of 22 patients in group 2 underwent pharmacologic stress testing with dipyridamole rather than treadmill stress testing. It is not generally recognized that the use of a coronary vasodilator agent can actually provoke a flow/demand mismatch and produce ischemia. In most patients, a coronary vasodilator uncovers reduced flow reserve in vascular beds perfused by stenotic lesions but does not provoke ischemia. However, in some patients with severe stenotic lesions and collateral flow to the distal bed, dipyridamole-induced increases in coronary flow may actually lead to a "steal phenomenon" in which increased flow in an adjacent bed can actually siphon flow away from the bed distal to a highly stenotic lesion through collateral channels, leading to an actual reduction in blood flow in the bed of the stenotic lesion, with resultant mismatch of flow and demand and consequent ischemia (19).

Edge detection. An alternative explanation for the reduction of post-stress LVEF in some patients with stress-induced ischemia relates to defect severity and the potential limitations of the edge detection algorithm in finding the correct endocardial edge when myocardial counts are severely reduced. Transmural myocardial thickening occurs primarily in the endocardial layer because the epicardium contributes little to thickening. The subendocardium is also the site of stress-induced ischemia. Although a theoretic limitation, it is unlikely that technical factors contributed to the findings in this study. The edge detection algorithm used in the present study and originally described by Germano et al. (16) identifies perfusion in underperfused areas of the myocardium by extracting count profiles from the nonthreshold image. Because the subendocardium is the site of stress-induced ischemia, and it can be assumed that related perfusion defects are localized predominantly to the endocardium, epicardial perfusion (albeit smoothed and reduced in intensity by the partial volume effect [20] and the relatively low resolution of the nuclear system) is seen in the count profiles. Moreover, an asymmetric gaussian is fitted to each profile, and the inner and outer standard deviations of the gaussian are measured. When perfusion is low along a profile, these standard deviations are automatically combined with those of each of its four spatial neighboring profiles (16). The endocardial and epicardial surfaces obtained are further refined by imposing the anatomic constraint of constant myocardial volume throughout the cardiac cycle.

Conclusions. The present study reports the observation that among a group of patients with stress-induced ischemia undergoing a two-day sestamibi imaging protocol, ~36% of patients had a post-stress LVEF, calculated using an automated program that detects the endocardial edge and calculates volume changes, that is below the lower bounds expected for the serial reproducibility of the measurement. The most likely explanation for this finding is the presence of postischemic stunning as a consequence of the stress-induced ischemic episode. The important practical and clinical implications of these findings are that the post-stress LVEF calculated using volume programs from the gated SPECT data cannot be considered to represent the basal LVEF value in all patients. The presence of postischemic reduction in the post-stress LVEF is probably another marker of disease severity and

probably a marker of reduced event-free survival, although further studies are needed to prove this premise.

References

1. Rozanski A, Elkayam U, Berman DS, Diamond GA, Prause J, Swan HJC. Improvement of resting myocardial asynergy with cessation of upright bicycle exercise. Circulation 1983;67:529–35.
2. Nixon JV, Brown CN, Smitherman TC. Identification of transient and persistent segmental wall motion abnormalities in patients with unstable angina by two-dimensional echocardiography. Circulation 1982;65:1497–503.
3. Rozanski A, Berman D, Gray R, et al. Preoperative prediction of reversible myocardial asynergy by postexercise radionuclide ventriculography. N Engl J Med 1982;307:212–6.
4. Ambrosio G, Betocchi S, Pace L, et al. Prolonged impairment of regional contractile function after resolution of exercise-induced angina: evidence of myocardial stunning in patients with coronary artery disease. Circulation 1996;94:2455–63.
5. Robertson S, Feigenbaum H, Armstong WF, Dillon JC, O'Donnell J, McHenry PW. Exercise echocardiography: a clinically practical addition in the evaluation of coronary artery disease. J Am Coll Cardiol 1983;2:1085–91.
6. Katz A, Force T, Folland E, Aebischer N, Sharma S, Parisi A. Echocardiographic assessment of ventricular systolic function. In: Marcus ML and Braunwald E, editors. Marcus Cardiac Imaging: a Companion to Braunwald's Heart Disease. Philadelphia: WB Saunders, 1996:297–324.
7. Heyndrickx GR, Millard RW, McRitchie RJ, Maroko PR, Vatner SF. Regional myocardial functional and electrophysiological alterations after brief coronary artery occlusion in conscious dogs. J Clin Invest 1975;56:978–85.
8. Theroux P, Ross J, Franklin D, Kemper WS, Sasyama S. Regional myocardial function in the conscious dog during acute coronary occlusion and responses to morphine, propranolol, nitroglycerin, and lidocaine. Circulation 1976;53:302–14.
9. Matsuzaki M, Gallagher KP, Kemper WS, White F, Ross J. Sustained regional dysfunction produced by prolonged coronary stenosis: gradual recovery after reperfusion. Circulation 1983;68:170–82.
10. Nicklas JM, Becker LC, Bulkley BH. Effects of repeated brief coronary occlusion on regional left ventricular function and dimension in dogs. Am J Cardiol 1985;56:473–8.
11. Vanoverschelde JL, Wijns W, Depre C, et al. Mechanisms of chronic regional postischemic dysfunction in humans. Circulation 1993;87:1513–23.
12. Dilsizian V, Bonow RO. Current diagnostic techniques of assessing myocardial viability in patients with hibernating and stunned myocardium. Circulation 1993;87:1–20.
13. Renkin J, Wijns W, Ladha Z, Col J. Reversal of segmental hypokinesis by coronary angioplasty in patients with unstable angina, persistent T wave inversion, and left anterior descending coronary artery stenosis. Circulation 1990;82:913–21.
14. Braunwald E, Kloner RA. The stunned myocardium prolonged, postischemic ventricular dysfunction. Circulation 1982;66:1146–9.
15. Kloner RA, Przyklenk K, Patel B. Altered myocardial states: the stunned and hibernating myocardium. Am J Med 1989;86:14–22.
16. Germano G, Kiat H, Kavanagh PB, et al. Automatic quantification of ejection fraction from gated myocardial perfusion SPECT. J Nucl Med 1995;36:2138–47.
17. Schwaiger M, Schelbert HR, Ellison D, et al. Sustained regional abnormalities in cardiac metabolism after transient in chronic dog model. J Am Coll Cardiol 1985;6:336–47.
18. Guth BD, Martin JF, Heusch G, Ross J Jr. Regional myocardial blood flow, function and metabolism using phosphorus-31 nuclear magnetic resonance spectroscopy during ischemia and reperfusion in dogs. J Am Coll Cardiol 1987;10:673–81.
19. Chambers CE, Brown KA. Dipyridamole-induced ST segment depression during thallium-201 imaging in patients with coronary artery disease: angiographic and hemodynamic determinants. J Am Coll Cardiol 1988; 12:37–41.
20. Hoffman E, Huang S, Phelps M. Quantitation in positron emission tomography: 1. effect of object size. J Comput Assist Tomogr 1979;3:299–308.